Effect of Temperature and Pressure on the Dynamic Miscibility of Hydrogen-Bonded Polymer Blends

K. Mpoukouvalas and G. Floudas*

Department of Physics, University of Ioannina, P.O. Box 1186, 451 10 Ioannina, Greece, and Foundation for Research and Technology-Hellas (FORTH), Biomedical Research Institute (BRI)

S. H. Zhang and J. Runt

Department of Materials Science and Engineering and Materials Research Institute, The Pennsylvania State University, University Park, Pennsylvania 16802

Received July 13, 2004; Revised Manuscript Received October 20, 2004

ABSTRACT: The dynamic miscibility of poly(4-vinylphenol)/poly(vinyl ethyl ether) (PVPh/PVEE) blends, with a T_g contrast of 186 K, as well as the PVEE segmental dynamics have been investigated by temperature- and pressure-dependent dielectric spectroscopy. In PVEE the pressure coefficient of T_g amounts to 0.215 K/MPa, and its apparent activation volume displays the usual T dependence. Although both temperature and volume contribute to the segmental dynamics, the former has a stronger influence within the T and P investigated. In the blends, dynamic heterogeneity is suppressed because of hydrogen bonds that couple the components' segmental dynamics. In the PVEE-rich blends, increasing temperature and pressure results in the broadening of the distribution of relaxation times through the weakening of hydrogen bonds and the associated decoupling of the segmental dynamics. A central result of the present study is the identification of a critical temperature above which the system becomes increasingly heterogeneous.

I. Introduction

Miscible polymer blends display a single—albeit broad—glass transition temperature (T_g) when examined by thermal methods (i.e., differential scanning calorimetry) but exhibit significant dynamic heterogeneity when examined by more "microscopic" methods such as NMR[1−3] and dielectric spectroscopy[4−6] or rheology.[4,7,8] The heterogeneity (i.e., the presence of "fast" and "slow" dynamics in a thermodynamically miscible blend) manifests itself as a different temperature dependence of the segmental relaxation times of the two components; the "fast" moving species relax with a rate comparable to the low-T_g component whereas the "slow" moving species with a rate intermediate between the two components. This dynamic heterogeneity was found to depend on the dynamic contrast between the two homopolymers, i.e., the difference in glass transition temperatures of the neat polymers (ΔT_g). Different models have been proposed to account for the dynamic heterogeneity in miscible polymer blends based on (i) intrinsic mobility differences,[1] (ii) local concentration fluctuations driven by the thermodynamic state,[9,10] and (iii) chain connectivity effects emphasizing the importance of a self-concentration in the blends.[11,12]

A way to compatibilize polymer blends is through specific interactions that effectively couple the components' dynamics. Recently, the component dynamics have been investigated in hydrogen-bonded blends[13−15] composed of poly(4-vinylphenol) (PVPh) as one component and poly(ethylene-*co*-vinyl acetate) (EVA)[14] or poly(vinyl ethyl ether) (PVEE)[15] as the second component. In these systems, the ability of intermolecular hydrogen bonding between the hydroxyl groups of PVPh and the carbonyl groups of EVA or the ether oxygen atoms in PVEE resulted in the coupling of the components' segmental dynamics, and this despite the extreme dynamic asymmetry based on the difference of the glass transition temperatures (ΔT_g of 173 and 186 K for the PVPh/EVA and PVPh/PVEE, respectively). Nevertheless, the coupling of the components' dynamics is not perfect. Two dielectrically active processes were found[15] for some compositions, called "fast" and "slow", reflecting respectively the dynamics of the unassociated (or "free") PVEE segments and of the intermolecular hydrogen-bonded PVPh and PVEE segments.

In the present investigation we employ pressure in addition to temperature and study the component dynamics in the PVPh/PVEE blends. Pressure has been employed earlier in two component systems. The first such study[16] dealt with the effect of pressure on the dynamic miscibility of the athermal block copolymer polyisoprene-*b*-poly(vinyl ethylene) (PI-*b*-PVE). The results of dielectric spectroscopy (DS) revealed that pressure reduces the dynamic heterogeneity, resulting in a dynamically (as well as thermodynamically) miscible system. The reason for this effect is the greater sensitivity to pressure of PI[17] as compared to PVE. The second system investigated was the polystyrene/poly(vinyl methyl ether) (PS/PVME).[18,19] In this system the dielectric activity of PVME is much higher than of PS, making the identification of the individual component dynamics a difficult task. The third system investigated was the PVPh/EVA hydrogen-bonded blend.[20] Despite the expected weakening of hydrogen bonds with increasing temperature and pressure, that would effectively decouple the components' segmental dynamics, the relaxation time distribution in the blends narrowed with increasing temperature and pressure when compared under isokinetic conditions. This rather unexpected result (given the higher sensitivity to pressure of PVPh[20] relative to EVA) was discussed in terms of an excess mobility gained by breaking hydrogen bonds at elevated T and P for the hydrogen-bonded PVPh/EVA segments.[20] Nevertheless, this effect was much smaller

10.1021/ma048585v CCC: $30.25
Published on Web 12/29/2004

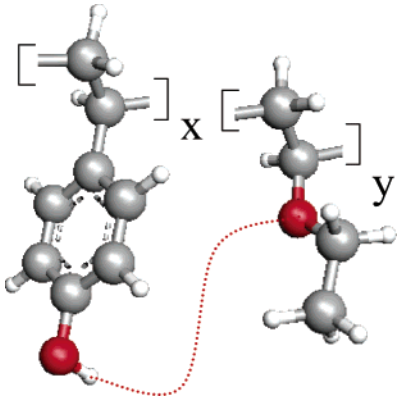

Figure 1. Schematic representation of the repeat units of PVPh and PVEE. The dotted line indicates the position of the intermolecular hydrogen bonds.

than in the PI-*b*-PVE system, despite the greater T_g contrast in the former system (ΔT_g of 173 of PVPh/EVA as compared to 60 K for PI-*b*-PVE) suggesting that hydrogen bonds play a dominant role in coupling the component dynamics in contrast to unassociated mixtures where the components can relax independently.

The PVPh/PVEE system employed herein exhibits a broadening of the relaxation time distribution by increasing temperature and pressure. Moreover, we show the existence of a critical temperature in blends rich in PVEE above which the (small) dynamic asymmetry is enhanced. In addition, we explore the origin of glass formation in PVEE by quantifying the relative contributions of temperature and volume on the segmental relaxation times.

II. Experimental Section

Samples. The PVPh (Polysciences, Inc.) with $M_w = 41\,000$ g/mol and $M_w/M_n = 6.8$ and the PVEE (Monomer-Polymer & DAJAC Laboratories, Inc.) with $M_w = 27\,000$ g/mol and $M_w/M_n = 2.1$ homopolymers are identical to the ones used in ref 15. Molecular weights were determined by gel permeation chromatography using poly(ethylene oxide) standards. Blends were prepared by solution casting from 5 wt % solutions of the neat polymers in methyl ethyl ketone. Figure 1 gives the repeat units of PVPh and PVEE, and the dotted line indicates the positions of hydrogen bonds.

Differential Scanning Calorimetry (DSC). A Seiko SSC 5200 DSC was used. The samples were heated to 50 K above the expected T_g and then cooled at a rate of 20 K/min. The samples were subsequently heated at a rate of 10 K/min, and T_g was obtained at the midpoint of the heat capacity change in the second heating run. The results on the glass transition temperatures from the second heating run are reported in Figure 2 as a function of the PVPh content. In the same figure the results from DS (T_g is operationally defined here as the temperature where the segmental relaxation time is at 10 s—this definition brings the homopolymer T_g in agreement with the DSC results) are included for comparison (see below).

Dielectric Spectroscopy (DS). The sample cell consisted of two electrodes with 20 mm in diameter and the sample with a thickness of 50 or 20 μm. The dielectric measurements were made at different temperatures in the range 123−453 K, at atmospheric pressure, and for frequencies in the range from 3×10^{-3} to 1×10^{6} Hz using a Novocontrol BDS system composed from a frequency response analyzer (Solartron Schlumberger FRA 1260) and a broadband dielectric converter. The complex dielectric permittivity $\epsilon^* = \epsilon' - i\epsilon''$, where ϵ' is the real and ϵ'' is the imaginary part, is a function of frequency ω, temperature T, and pressure P, $\epsilon^* = \epsilon^*(\omega,T,P)$. In Figure 3, some representative dielectric permittivity and the corresponding loss spectra are shown for the pure PVEE under

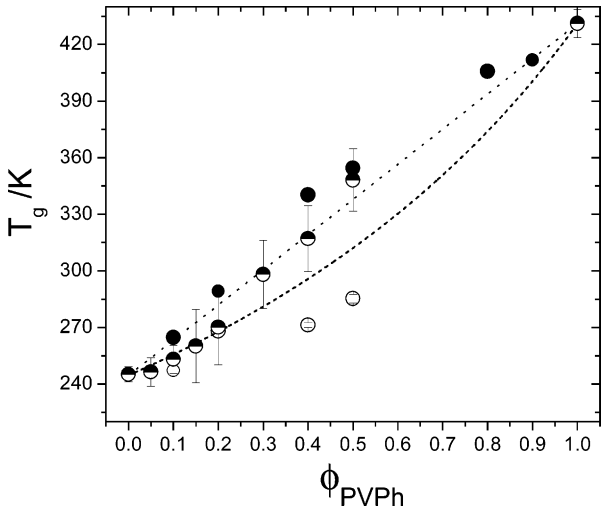

Figure 2. Dependence of the glass transition temperatures on PVPh content in the PVPh/PVEE blends. The single DSC T_g is shown with half-filled symbols together with the DSC ΔT_g range. The results from the DS study are shown with open and filled symbols for the "low" and "high" T_g, respectively (see text). The dotted line indicates a linear dependence whereas the dashed line is the prediction of the Fox−Flory equation (see text). Note that the "low" T_g is located below the predictions from the Fox−Flory equation whereas the "high" T_g is situated above the linear composition dependence. The latter is characteristic of hydrogen-bonded systems. Note that the DSC T_g is located between the "high" and "low" DS T_g's.

"isobaric" (left) and "isothermal" (right) conditions. In the analysis of the DS spectra we have used the empirical equation of Havriliak and Negami (HN):[21]

$$\frac{\epsilon^*(T,P,\omega) - \epsilon_\infty(T,P)}{\Delta\epsilon(T,P)} = \frac{1}{[1 + (i\omega\tau_{HN}(T,P))^\alpha]^\gamma} \qquad (1)$$

where $\tau_{HN}(T,P)$ is the characteristic relaxation time in this equation, $\Delta\epsilon(T,P) = \epsilon_0(T,P) - \epsilon_\infty(T,P)$ is the relaxation strength of the process under investigation, and α and γ (with limits $0 < \alpha$, $\alpha\gamma \leq 1$) describe respectively the symmetrical and asymmetrical broadening of the distribution of relaxation times. In the fitting procedure we have used the ϵ'' values at every temperature, and in some cases the ϵ' data were also used as a consistency check.

The linear rise of the ϵ'' at lower frequencies is caused by the conductivity ($\epsilon'' \sim (\sigma_o/\epsilon_f)\omega^{-1}$, where σ_0 is the dc conductivity and ϵ_f is the permittivity of free space) which has been included in the fitting procedure. From τ_{HN}, the relaxation time at maximum loss, τ_{max}, is obtained analytically following

$$\tau_{max} = \tau_{HN}\left[\frac{\sin\left(\frac{\pi\alpha}{2+2\gamma}\right)}{\sin\left(\frac{\pi\alpha\gamma}{2+2\gamma}\right)}\right]^{-1/\alpha} \qquad (2)$$

For the neat PVPh and the blends rich in PVPh there is a strong conductivity contribution. In these cases we have used the first derivative method of ϵ' to derive the ϵ'' as $\epsilon''_{calc} = -(\pi/2)(\partial\epsilon'/\partial \ln \omega)$, which provides an ohmic conduction free dielectric loss.[22]

III. Results and Discussion

In the DSC experiment (Figure 2), very broad transition regimes around the single blend T_g were found, especially for the blends rich in PVEE (the vertical lines indicate the DSC transition regime, ΔT_g). In the same figure the DS results are shown for the two processes in the blends. The "fast" (low T_g) and "slow" (high T_g)

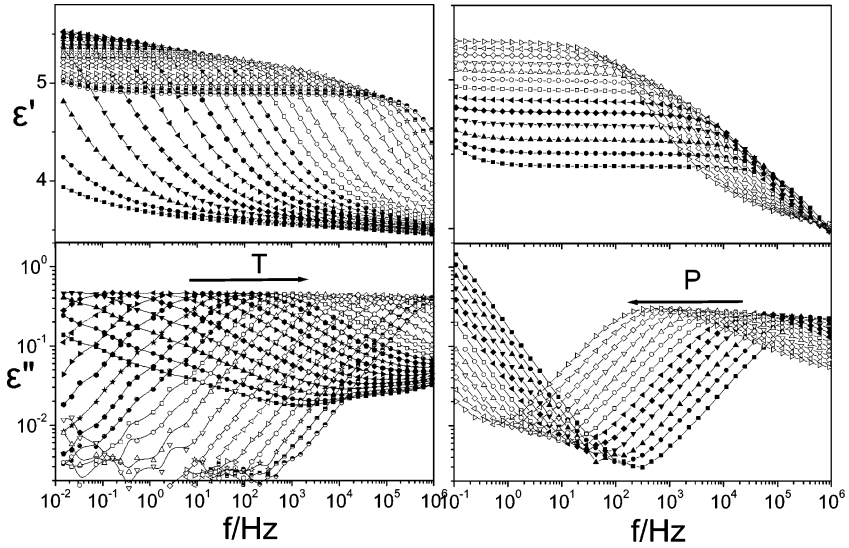

Figure 3. Dielectric permittivity (top) and dielectric loss (bottom) curves for neat PVEE, at atmospheric pressure, for different temperatures in the range from 268.15 to 314.15 K (left) and at 309.15 K for different pressures in the range from 20 to 260 MPa (right).

processes in the blends with $\varphi_{PVPh} \leq 0.5$ are associated with the dynamics of nearly free (i.e., unassociated) PVEE segments and coupled relaxation of PVEE and PVPh segments through hydrogen bonds. The corresponding processes in the blends with $0.5 < \varphi_{PVPh} < 0.8$ display a similar trend; however, spectral decomposition in this regime becomes increasingly difficult, suggesting a more homogeneous dynamic environment in this intermediate composition regime. In the blends with $\varphi_{PVPh} \geq 0.8$, because of intensity reasons, only the high-T_g component can be unambiguously obtained. In the same figure, the predictions from the Fox−Flory equation ($T_g^{-1} = \varphi T_{g1}^{-1} + (1 - \varphi)T_{g2}^{-1}$) and of a linear composition dependence ($T_g = \varphi T_{g1} + (1 - \varphi)T_{g2}$) are shown. Note that the "low" and "high" DS glass temperatures are located below and above the Fox−Flory and linear predictions, respectively. The weak $T_g(\varphi)$ dependence corresponding to the "fast" process (i.e., the low T_g process) reveals a PVEE-rich environment in the blends similar to that found in polymer/diluent systems, whereas the $T_g(\varphi)$ dependence of the "slow" process (i.e., the high-T_g process) is the norm for hydrogen-bonded systems exhibiting an increased glass temperature as a result of the imposed constraints. Interestingly, the DSC T_g for low PVPh content follows the Fox−Flory equation whereas for intermediate compositions it follows the linear composition relation. In any case, DSC is incapable of differentiating between the different segmental mobilities present in the blends.

DS, on the other hand, is a very sensitive probe of the local environment and provides the means of exploring the dynamic heterogeneity in polymer blends. First, we briefly discuss the homopolymer dynamics. The "isobaric" and "isothermal" dielectric loss data of the PVEE homopolymer shown in Figure 3 reveal a main (α-) process and a secondary (β-) process at the high-frequency side of the "isobaric" data. In addition, the "isothermal" dielectric permittivity curves reveal an isosbestic point at $f \sim 7 \times 10^5$ Hz, revealing the contribution from two processes (α- and β-) with different T dependencies. These curves have been shifted to the α-process loss maximum of the corresponding reference "isothermal" and "isobaric" curves as shown in Figure 4. In the shifting procedure the frequency axis of each curve has been multiplied by appropriate horizontal (and vertical) shift factors a_T (b_T) and a_P (b_P), at each T and P. The T and P dependence of the vertical shift factors (with slopes $db_T/dT = 1.8 \times 10^{-3}$ K^{-1} and $db_P/dP = 1.1 \times 10^{-3}$ MPa^{-1}) are shown in the insets. The resulting master curves suggest that time−temperature−pressure superposition (tTPs) works reasonably well for PVEE within the examined T and P ranges. The deviations at low and high frequencies are caused by contributions from the conductivity and the faster β-process, respectively. The latter has a weak T and P dependence and will not be discussed here in detail. The α and γ Havriliak−Negami shape parameters for the segmental process in PVEE are $\alpha = 0.77 \pm 0.03$ and $\gamma = 0.49 \pm 0.03$, respectively. The corresponding parameters for PVPh are 0.6 ± 0.1 and 0.9 ± 0.1, respectively. Furthermore, the dielectric strength ($\Delta\epsilon$) of the α-process can be used to estimate the effective dipole moment, from $\Delta\epsilon \sim (\mu^2/3k_BTV)FgN$, where μ is the dipole moment, V is the volume, N is the number of dipoles, F is a local field correction ($F = 3.9$ and 3.2 for PVEE and PVPh, at the respective T_g), and g is the Kirkwood−Fröhlich angular correlation factor. The effective dipole moment thus calculated ($\mu_{eff} = (g\mu^2)^{1/2}$) amounts to 0.71 and 0.85 for PVEE and PVPh, respectively. These values are substantially lower than in the corresponding small molecule analogues in benzene (1.25 and 1.61 D, respectively).

All $\tau(T)$ dependencies conform to the well-known Vogel−Fulcher−Tammann (VFT) equation

$$\tau_{max} = \tau_0 \exp\left(\frac{D_T T_0}{T - T_0}\right) \quad (3)$$

where τ_0 is the relaxation time at practically infinite T, D_T is a dimensionless parameter, and T_0 is the "ideal" glass temperature.

Subsequently, we examined the pressure dependence of the dynamics in the two homopolymers. The results for the relaxation times at maximum loss of bulk PVEE are shown in Figure 5 as a function of pressure. The good linearity within the investigated P range suggests that each T is associated with an apparent

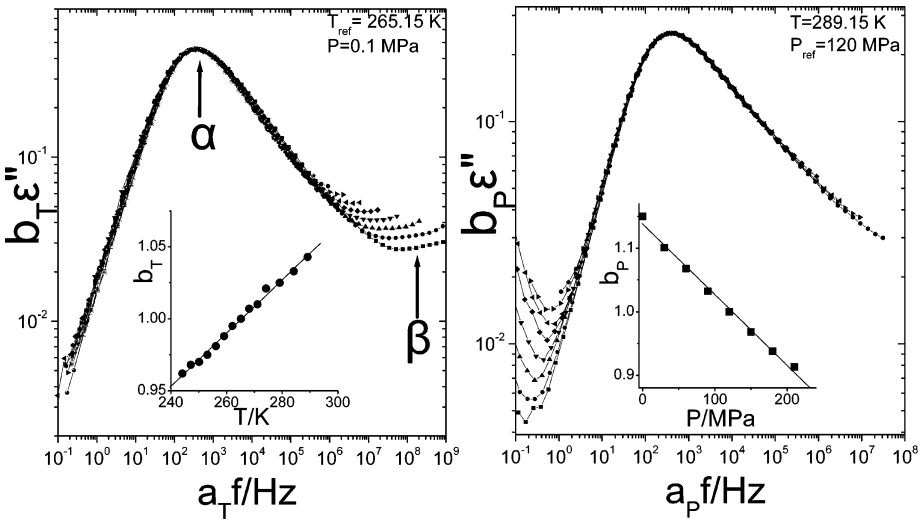

Figure 4. (left) Master curve construction using time−temperature superposition (tTS) for the "isobaric" dielectric loss data of neat PVEE. The arrows indicate the position of the α- and β-processes. (right) Master curve construction using time−pressure superposition for the "isothermal" data of neat PVEE. The T and P dependencies of the vertical shift factors b_T and b_P are shown in the insets.

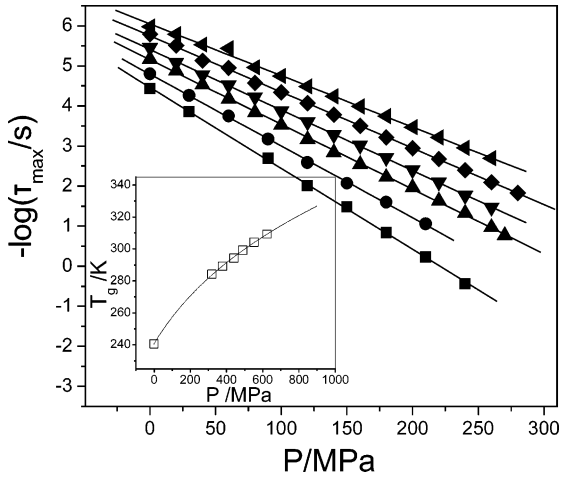

Figure 5. Pressure dependence of the relaxation times at maximum loss for the α-process of neat PVEE plotted for different temperatures: (■) $T = 284.15$ K, (●) $T = 289.15$ K, (▲) $T = 294.15$ K, (▼) $T = 299.15$ K, (◆) $T = 304.15$ K, (tilted ▲) $T = 309.15$ K. The lines are the result of the fit giving rise to the apparent activation volume according to eq 4. In the inset the $T_g(P)$ dependence for PVEE (open symbols). The line is the result of the fit to eq 5 on the PVEE data.

activation volume,[19] according to

$$\Delta V = 2.303RT\left(\frac{\partial \log \tau}{\partial P}\right)_T \tag{4}$$

The resulting ΔV displays a strong T dependence, and this feature will be discussed later with respect to Figure 13. From $\tau(P)$, the $T_g(P)$ dependence can be extracted using the operational definition of T_g (by linear extrapolation to $\tau = 10$ s). The $T_g(P)$ dependence for PVEE is shown in the inset to Figure 5 and can be described by the empirical equation[23,24]

$$T_g(P) = T_g(0)\left(1 + \frac{b}{c}P\right)^{1/b} \tag{5}$$

where $T_g(0)$ is the glass transition temperature at atmospheric pressure and b, c are constants. These parameters for PVEE are $T_g(0) = 240.6 \pm 0.5$ K, $b = 5.9 \pm 0.3$, and $c = 1119 \pm 50$ MPa, and the initial slope, $(dT_g/dP)_{P\to 0} = T_g(0)/c$, amounts to 0.215 K/MPa.

Pressure, apart from influencing the segmental relaxation times and the associated glass temperature, can be employed as the relevant thermodynamic variable in the discussion of the origin of glass formation.[25] The origin of the slowing down of the dynamics by decreasing temperature toward T_g has been discussed in terms of two different models. According to the first model,[26] glass formation is associated with the decrease of the available (or "free") volume. According to the second model,[27] glass formation is the result of trapping within the potential energy surface through the decrease in the thermal energy (k_BT). Since decreasing T affects both thermal energy and the available volume, T alone cannot differentiate between the proposed models. On the other hand, pressure can be applied isothermally and thus provides the means of extracting the relative contribution of V and T on the glass formation. To quantify the relative effect of volume and thermal energy, we employ the constant volume activation energy $E_V = R(\partial \ln \tau/\partial T^{-1})_V$ and the constant pressure activation energy $E_P = R(\partial \ln \tau/\partial T^{-1})_P$. The ratio E_V/E_P is a direct measure of the relative contribution of temperature and volume to the relaxation times.[28−34] Then the absence of an activation energy under conditions of constant volume (i.e., $E_V \to 0$) would imply that volume is the only controlling parameter of the segmental dynamics whereas values of the ratio close to one would suggest that T is the main controlling parameter of the dynamics. The ratio of activation energies can be obtained experimentally or calculated through[30]

$$\frac{E_V}{E_P} = 1 - \left(\frac{\partial P}{\partial T}\right)_V\left(\frac{\partial T}{\partial P}\right)_\tau \tag{6}$$

where $(\partial P/\partial T)_V$ can be calculated from PVT data and $(\partial T/\partial P)_\tau$ is the pressure coefficient of T_g. To obtain this ratio for PVEE, we employ the Tait equation of state:[35]

$$V(P,T) = V(0,T)\left\{1 - 0.0894 \ln\left[1 + \frac{P}{B(T)}\right]\right\} \tag{7}$$

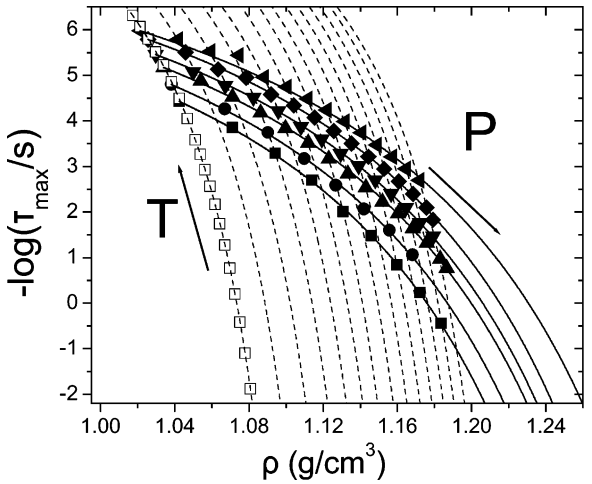

Figure 6. Dependence of the "isothermal" (solid lines) and "isobaric" (dashed lines) relaxation times on density of neat PVEE. The lines are the result of the fits to eq 8 with $D_\rho^T = 5.87$ and $D_\rho^P = 1.16$, respectively. The different "isotherms" correspond to the following temperatures: (■) $T = 284.15$ K, (●) $T = 289.15$ K, (▲) $T = 294.15$ K, (▼) $T = 299.15$ K, (◆) $T = 304.15$ K, (tilted ▲) $T = 309.15$ K. The "isobaric" data at $P = 0.1$ MPa are shown with open squares.

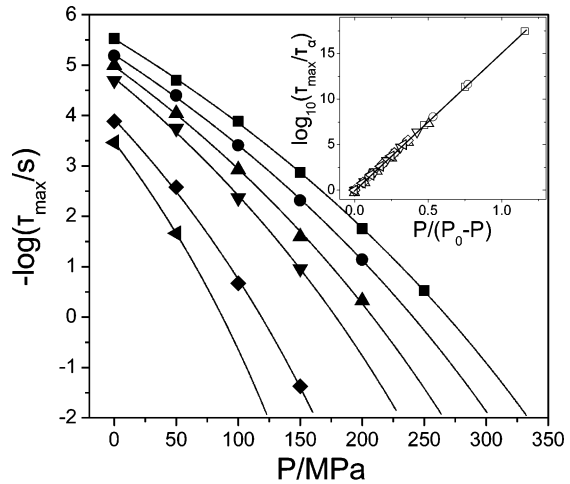

Figure 7. Pressure dependence of the relaxation times at maximum loss for the main α-process in the PVPh/PVEE (50/50) blend at different temperatures: (■) $T = 409.15$ K, (●) $T = 403.15$ K, (▲) $T = 398.15$ K, (▼) $T = 393.15$ K, (◆) $T = 383.15$ K, (tilted ▲) $T = 378.15$ K. The lines are fits to the modified VFT equation for pressure (eq 9). In the inset the reduced relaxation times are plotted as a function of reduced pressures for the different "isotherms". Note the good linearity according to eq 9.

where $V(0,T) = A_0 + A_1T$ is the specific volume at atmospheric pressure and $B(T) = B_0 \exp(-B_1T)$. The following parameters were obtained from the PVT measurements of PVEE: $A_0 = 0.95$ cm^3/g, $A_1 = 7.94 \times 10^{-4}$ cm^3/(°C g) and $B_0 = 88$ MPa, $B_1 = 2.26 \times 10^{-3}$ °C^{-1}. With these parameters the $\tau(T,P)$ dependencies can be transformed into a single $\tau(\rho)$ dependence ($\rho = V^{-1}$). The result of this transformation for PVEE is shown in Figure 6. The plot depicts both the "isothermal" and the "isobaric" relaxation times, and the solid and dashed lines are the fits to the modified VFT equation:[19]

$$\tau_{\max} = \tau_0 \exp\left(\frac{D_\rho \rho}{\rho_0 - \rho}\right) \tag{8}$$

where D_ρ is a dimensionless parameter and ρ_0 is the density of the "ideal" glass. From the intersection points of the "isothermal" (with $D_\rho^T = 3.14$) and "isobaric" (with $D_\rho^P = 1.47$) lines, the ratio E_V/E_P can be readily obtained. This ratio for PVEE is within the range from 0.72 to 0.82 for the different temperatures and pressures investigated. The same ratio can be calculated through eq 6 and amounts to 0.81 for $\tau \sim 1$ s. Therefore, both temperature and volume play a role in determining the segmental relaxation times, with the former having a stronger influence (especially at low T and P).

The strong conductivity contribution in the other homopolymer (PVPh) and in the blends rich in PVPh precludes a P-dependent investigation. We therefore concentrate on the effect of pressure on the blends with $\varphi_{\mathrm{PVPh}} \leq 0.5$. Figure 7 gives the P dependence of the intense slower mode in the PVPh/PVEE (50/50) blend corresponding to the hydrogen-bonded segments. In contrast to the linear $\tau(P)$ dependence found in bulk PVEE, the process displays a strong P dependence that can be parametrized according to the modified VFT for P dependence:

$$\tau_{\max} = \tau_\alpha \exp\left(\frac{D_P P}{P_0 - P}\right) \tag{9}$$

where τ_α is the segmental relaxation time at atmospheric pressure at a given T, D_P is a dimensionless parameter, and P_0 is the "ideal" glass pressure. All isothermal relaxation times conform to eq 9 as shown by the scaling of the reduced relaxation times plotted as a function of reduced pressure in the inset to Figure 7 (with a slope of $D_P = 34.7$). The P dependence of the "fast" process is weak, and this process will be discussed later with respect to the PVPh/PVEE (10/90) blend.

In the blends with high PVEE content, the DS curves became more asymmetric and under certain T, P conditions, bimodal. This is shown in Figure 8 for the PVPh/PVEE (10/90) blend under "isobaric" (left) and "isothermal" (right) conditions. The figure displays the curves shifted to reference conditions of $T = 293.15$ K and $P = 100$ MPa, respectively, and show the breakdown of time−temperature−pressure superposition (tTPs) in sharp contrast to the PVEE homopolymer. Furthermore, increasing T and P produce opposite effects on the broadening of the dielectric loss spectra: increasing T results in more narrow and symmetric curves whereas increasing P results in broader and more asymmetric loss curves. In the fitting procedure we have used two HN functions in addition to the conductivity contribution. The blend shape parameters for the "fast" and "slow" processes are, in general, lower (i.e., broader curves) than in the homopolymers as a result of local concentration fluctuations.[9]

In Figure 9, the dielectric loss curves of the PVPh/PVEE (10/90) blend recorded at different (T, P) combinations are compared under different isokinetic conditions. The blend data have been slightly shifted vertically to match the $\epsilon''_{\max}$ values, but not horizontally. The data show an increasing slope in the high-frequency side at $T > 294$ K. This finding suggests increasing strength of the faster α-process corresponding to PVEE segmental relaxation at the expense of the slower α-process corresponding to hydrogen-bonded PVPh and PVEE segments. Thus, the raw data suggest increasing heterogeneity above 294 K. At and below 294 K, the relaxation time distributions do not change at different isokinetic (T, P) combinations. (There may even be a

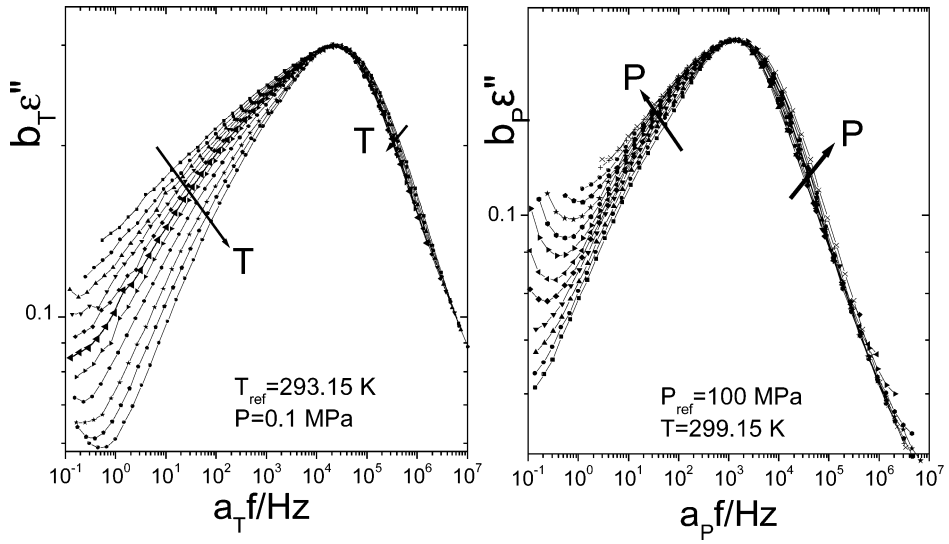

Figure 8. (left) Master curve construction using the time−temperature superposition (tTs) for temperatures in the range from 275.15 to 313.15 K and (right) using the time−pressure superposition, for pressures in the range from 0.1 to 240 MPa, for the PVPh/PVEE (10/90) blend. Arrows indicate the trend for increasing T and P. Notice the breakdown of both tTs and tPs in the 10/90 blend.

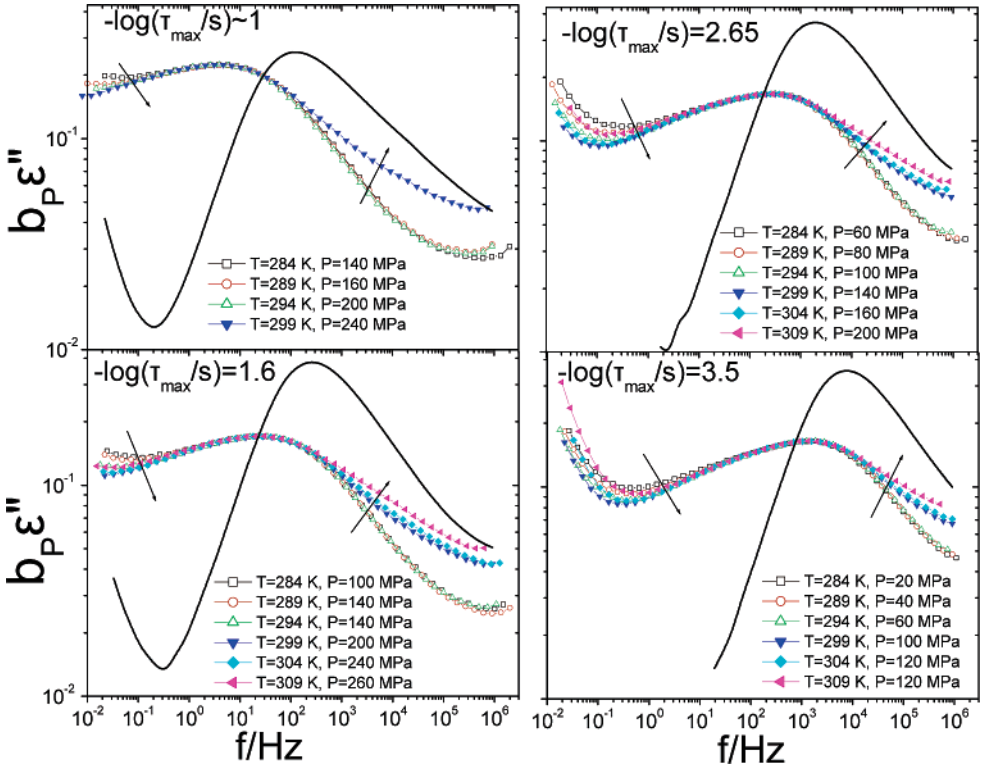

Figure 9. Comparison of some isokinetic (T, P) sets of dielectric loss curves for the PVPh/PVEE (10/90) blend at different times as indicated. The solid lines give the PVEE dielectric loss curves at T = 289.15 K, P = 150 MPa (for $-\log(\tau_{max}/s) = 1$), at T = 299.15 K, P = 200 MPa (for $-\log(\tau_{max}/s) = 1.6$), at T = 299.15 K, P = 140 MPa (for $-\log(\tau_{max}/s) = 2.65$) and at T = 299.15 K, P = 100 MPa (for $-\log(\tau_{max}/s) = 3.5$). Note the change in the blend curves at T = 294 K.

slight narrowing on the low-frequency side with increasing (T, P) at the same relaxation time, similar to previous results for the PVPh/EVA blend.[20]) To quantify this effect on the segmental dynamics and the associated populations, we show in Figure 10 the $\tau(P)$ for both processes under different "isothermal" conditions. The results for the dynamics reveal a linear $\tau(P)$ dependence for the fast (open symbols) and the slow (filled symbols) processes in the PVPh/PVEE (10/90) blend with slightly different slopes (we will return to the slopes, i.e., apparent activation volumes, later with respect to Figure 13). Clearly, the dynamics speed up above 294 K. This finding for the dynamics finds its counterpart in the associated dielectric strengths. The corresponding strength ($T\Delta\epsilon$) for the slower process is plotted in Figure 11 for the same data shown in Figure 10. Again at $T >$ 294 K, the slower process loses in strength with a magnitude that depends on thermal history. Therefore, both $\tau(P)$ and $\Delta\epsilon(P)$ results indicate the existence of a critical temperature at $T_c \sim 294$ K.

The existence of the critical temperature is better demonstrated in a $T-P$ representation under different isokinetic conditions as shown in Figure 12. Such a diagram can be made for both the "slow" and the "fast"

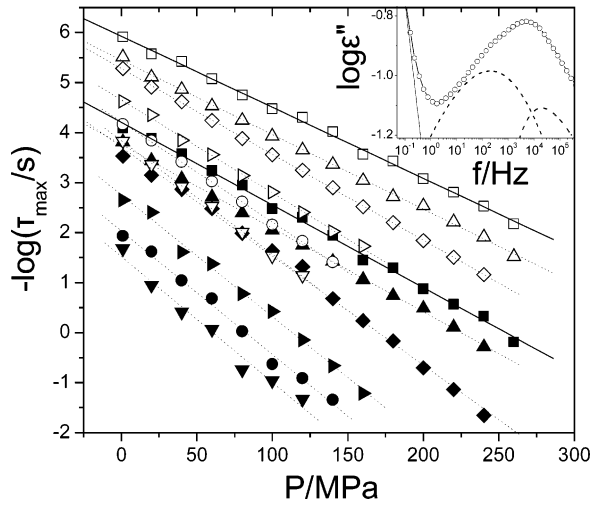

Figure 10. Pressure dependence of the relaxation times of the PVPh/PVEE (10/90) blend corresponding to the "fast" (open symbols) and "slower" (filled symbols) processes at selected temperatures: (■, □) T = 309.15 K, (▲, △) T = 304.15 K, (◆, ◇) T = 299.15 K, (tilted ▲, tilted △) T = 294.15 K, (●, ○) T = 289.15 K, (▼, ▽) T = 284.15 K. Lines are the result of linear fits according to eq 4. In the inset, a fitting example to a bimodal HN function is shown (at T = 309 K, P = 120 MPa).

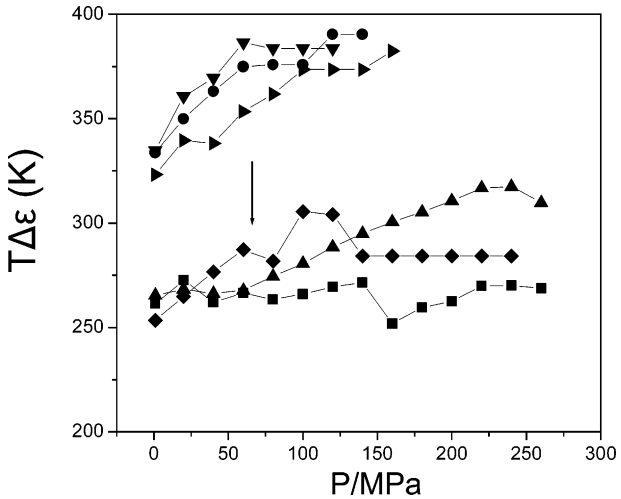

Figure 11. Pressure dependence of the dielectric strength ($T\Delta\epsilon$) for the "slow" process in the PVPh/PVEE (10/90) blends plotted for the same temperatures as in Figure 10: (■) T = 309.15 K, (▲) T = 304.15 K, (◆) T = 299.15 K, (tilted ▲) T = 294.15 K, (●) T = 289.15 K, (▼) T = 284.15 K. The vertical arrow indicate the changes at $T \sim 294$ K.

processes in the blend—the results depicted in the figure refer to the slower α-process for PVPh/PVEE 10/90. Independent of the chosen times, the isokinetic curves reveal a change in the slope dT/dP at 294 K as anticipated from the dynamic response (Figure 10) and the associated populations (Figure 11). For example, dT/dP changes from 0.17 at T < 294 K, to 0.1 at $T \sim 294$ K, and back to 0.17 K/MPa at T > 294 K. Given that away from first-order transitions (i.e., under constant volume conditions) dT/dP is given by the ratio κ_T/β (k_T is the isothermal compressibility and β is the thermal expansion coefficient), the results suggest a different material within a narrow T range around 294 K.

The presence of a critical temperature is not uncommon for hydrogen-bonded systems. For example, PEO/water solutions exhibit an enthalpy driven lower critical solution temperature that separates a hydrogen-bonded single-phase region at low temperatures from a two-phase region at higher temperatures.[36−38] The system is thought to mix through hydrogen bonds and to demix when hydrogen bonds weaken. Furthermore, the effect of hydrostatic pressure[37] is to lower the LCST by breaking the "geometrically sensitive"[39] hydrogen bonds. In the present case, T rather than P is the dominant factor giving rise to the breaking of hydrogen bonds since within the investigated range pressure does not seem to alter T_c (Figure 9).

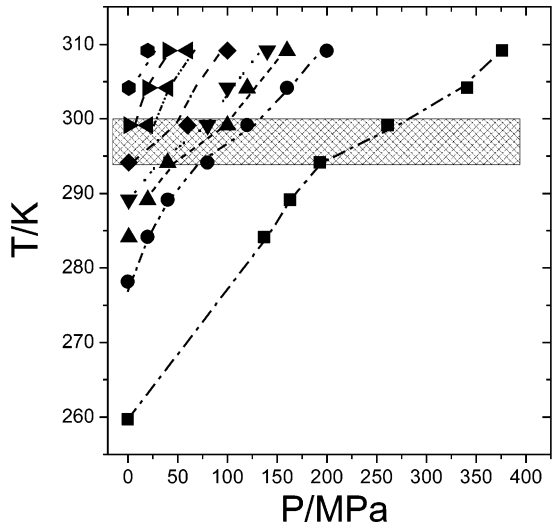

Figure 12. $T-P$ representation for the isokinetic lines corresponding to the "slow" process in the PVPh/PVEE (10/90) blend. The different symbols correspond to the following times: (■) $-\log(\tau_{max}/s) = -2$, (●) $-\log(\tau_{max}/s) = 1$, (▲) $-\log(\tau_{max}/s) = 1.6$, (▼) $-\log(\tau_{max}/s) = 2$, (◆) $-\log(\tau_{max}/s) = 2.65$, (left tilted ▲) $-\log(\tau_{max}/s) = 3.1$, (right tilted ▲) $-\log(\tau_{max}/s) = 3.5$, and (⬢) $-\log(\tau_{max}/s) = 3.75$. Note the change in slope at $T \sim 294$ K.

The $T_g(P)$ dependencies for the different processes in the blends can be described by eq 5 as for the PVEE homopolymer. The initial slopes for the "fast" and "slow" processes in the PVEE/PVPh (90/10) are 0.193 and 0.207 K/MPa, respectively. For the PVEE/PVPh (80/20) blend the corresponding values are 0.21 and 0.226 K/MPa, respectively. Notice the similarity of the slopes for the two processes that is expected on the basis of the homopolymer dependencies $((dT_g/dP)_{P\to 0}$ amounts to 0.215 and 0.225 K/MPa for PVEE and PVPh[20] homopolymers, respectively.

At this point, we employ the apparent activation volume through the $\tau(P)$ dependence and compare the different processes in the PVPh/PVEE 10/90, 20/80, and 50/50 blends with the neat PVEE. The comparison is made in Figure 13 as a function of the temperature difference from the respective T_g. Notice that the small difference in the apparent activation volumes for the "fast" and "slow" processes in the PVEE-rich blends (Figure 10) is lost in the T_g-scaled representation. Furthermore, the close proximity of the "fast" blend component apparent activation volumes to the bulk PVEE data suggests nearly pure PVEE segmental relaxation. Furthermore, in the blends rich in PVEE, $\Delta V_{fast} \sim \Delta V_{slow}$, suggesting that the dynamics of the slower process are also controlled by the fast moving species (PVEE). For the PVEE/PVPh 50/50 blend, the higher ΔV could reflect the higher values of PVPh.[20]

Last we comment on the different dynamic response of the EVA/PVPh blends with respect to the PVEE/PVPh blends. In the former system the DS curves became narrower with increasing P, whereas the op-

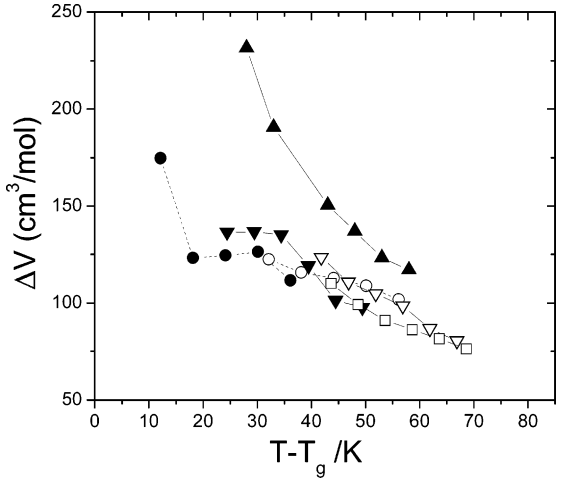

Figure 13. Apparent activation volume as a function of temperature difference from the respective T_g: (□) PVEE, (▼, ▽) "slow" and "fast" components of PVPh/PVEE (10/90), (●, ○) "slow" and "fast" components of the PVPh/PVEE (20/80) blend, and (▲) the PVPh/PVEE (50/50) blend.

posite is the case in the latter at $T > 294$ K (Figure 9). This is despite the similar T_g contrast between PVPh with PVEE and EVA (186 and 173 K, respectively). However, the hydrogen bond strength is significantly different: 5.4 vs 3.8 kcal/mol for PVPh/PVEE and PVPh/EVA, respectively. The stronger hydrogen bonding between PVEE and PVPh contributes significantly to the enthalpy of mixing, and we propose that this contribution decreases relatively quickly with temperature and leads to a critical temperature at $T \sim 294$ K. For PVPh/EVA blends, however, the intermolecular hydrogen bonding is relatively weak, and the change in the corresponding mixing enthalpy with T is presumably insufficient to induce a critical temperature at the temperatures and pressures studied.

IV. Conclusions

We have investigated the effects of temperature and pressure on neat PVEE dynamics and in hydrogen-bonded blends of PVEE with PVPh.

With respect to the neat PVEE we found that the segmental relaxation obeys time−temperature−pressure superposition. Using pressure, we identified the pressure coefficient of T_g as $(dT_g/dP)_{P\to 0} = 0.215$ K/MPa, the T-dependent apparent activation volume (with $\Delta V \sim 100$ cm^3/mol at $T = T_g + 50$ K), and the ratio of activation energies, E_V/E_P, range from 0.72 to 0.82 for the different T and P investigated. The latter implies that both temperature and volume are important parameters, giving rise to the dynamic arrest at T_g; however, since this value is significantly above 0.5, temperature has a stronger influence on the segmental dynamics.

The dynamic heterogeneity in the blends is reduced relative to other systems with a high ΔT_g difference due to hydrogen bonding that couples the components' segmental dynamics. Increasing temperature and pressure results in the broadening of the distribution of relaxation times through the weakening of hydrogen bonds and the associated decoupling of the segmental dynamics. The main results from the P- and T-dependent investigation are the following:

(i) Both the dynamics and the associated populations of the "fast" and "slow" processes in the PVEE-rich blends revealed the existence of a critical temperature which is reminiscent to the lower critical solution temperature found in other hydrogen-bonded systems (i.e., PEO/water). However, in the present system above this temperature the system becomes more, but not completely, heterogeneous as one would anticipate from a purely thermodynamic LCST.

(ii) The apparent activation volume associated with the "fast" process in the PVEE-rich blends is indistinguishable from neat PVEE. Furthermore, $\Delta V_{slow} \sim \Delta V_{fast}$, suggesting that the $\tau(P)$ for both processes are controlled by the fast moving species (i.e., the PVEE).

Acknowledgment. K.M. and G.F. acknowledge support by the Program PENED01 (GSRT). The Penn State authors express their appreciation to the National Foundation, Polymers Program (DMR-0211056), for support of this research. We are thankful to A. Best (MPI-P) for the PVT measurements.

References and Notes

(1) Chung, G.-C.; Kornfield, J. A. *Macromolecules* **1994**, *27*, 964.
(2) Miller, J. B.; McGrath, K. J.; Roland, C. M.; Trask, C. A.; Garroway, A. N. *Macromolecules* **1990**, *23*, 4543.
(3) Roland, C. M.; Ngai, K. L. *Macromolecules* **1992**, *25*, 363.
(4) Pathak, J. A.; Colby, R. H.; Floudas, G.; Jerome, R. *Macromolecules* **1999**, *32*, 2553.
(5) Kamath, S.; Colby, R. H.; Kumar, S. K.; Karatasos, K.; Floudas, G.; Fytas, G.; Roovers, J. *J. Chem. Phys.* **1999**, *111*, 6121.
(6) Arbe, A.; Alegria, A.; Colmenero, J.; Hoffmann, S.; Willner, L.; Richter, D. *Macromolecules* **1999**, *32*, 7572.
(7) Roovers, J.; Toporowski, P. M. *Macromolecules* **1992**, *25*, 1096.
(8) Pathak, J. A.; Colby, R. H.; Kamath, S. Y.; Kumar, S. K.; Stadler, R. *Macromolecules* **1998**, *31*, 8988.
(9) Zetsche, A.; Fischer, E. W. *Acta Polym.* **1994,** *45*, 168.
(10) Kumar, S.; Colby, R. H.; Anastasiadis, S. H.; Fytas, G. *J. Chem. Phys.* **1996**, *105*, 3777.
(11) Lodge, T. P.; McLeish, T. C. B. *Macromolecules* **2000**, *33*, 5278.
(12) Kant, R.; Kumar, S. K.; Colby, R. H. *Macromolecules* **2003**, *36*, 10087.
(13) Zhang, S. H.; Jin, X.; Painter, P. C.; Runt, J. *Macromolecules* **2002**, *35*, 3636.
(14) Zhang, S.; Painter, P. C.; Runt, J. *Macromolecules* **2002**, *35*, 8478.
(15) Zhang, S.; Painter, P. C.; Runt, J. *Macromolecules* **2002**, *35*, 9403.
(16) Floudas, G.; Fytas, G.; Reisinger, T.; Wegner, G. *J. Chem. Phys.* **1999**, *111*, 9129.
(17) Floudas, G.; Gravalides, C.; Reisinger, T.; Wegner, G. *J. Chem. Phys.* **1999**, *111*, 9847.
(18) Alegria, A.; Gomez, D.; Colmenero, J. *Macromolecules* **2002**, *35*, 2030.
(19) Floudas, G. In *Broadband Dielectric Spectroscopy*; Kremer, F., Schoenhals, A., Eds.; Springer: Berlin, 2002; Chapter 8.
(20) Zhang, S. H.; Casalini, R.; Runt, J.; Roland, C. M. *Macromolecules* **2003**, *36*, 9917.
(21) Havriliak, S.; Negami, S. *Polymer* **1967**, *8*, 161.
(22) Wübbenhorst, M.; van Koten, E.; Jansen, J.; Mijs, M.; van Turnhout, J. *Macromol. Rapid Commun.* **1997**, *18*, 139.
(23) Andersson, S. P.; Andersson, O. *Macromolecules* **1998**, *31*, 2999.
(24) Casalini, R.; Roland, C. M. *J. Chem. Phys.* **2003**, *119*, 4052.
(25) Ferrer, M. L.; Lawrence, C.; Demirjian, B. G.; Kivelson, D.; Alba-Simionesco, C.; Tarjus, G. *J. Chem. Phys.* **1998**, *109*, 8010.
(26) Ferry, J. D. In *Viscoelastic Properties of Polymers*, 3rd ed.; Wiley: New York, 1980.
(27) Angell, C. A. *Science***1995**, *267*, 1924.
(28) Williams, G. *Trans. Faraday Soc.* **1964**, *60*, 1556.
(29) Williams, G. *Trans. Faraday Soc.* **1966**, *62*, 2091.
(30) Naoki, M.; Endou, H.; Matsumoto, K. *J. Phys. Chem.* **1987**, *91*, 4169.
(31) Paluch, M.; Pawlus, S.; Roland, C. M. *Macromolecules* **2002**, *35*, 7338.

(32) Mpoukouvalas, K.; Floudas, G. *Phys. Rev. E* **2003**, *68*, 031801.
(33) Kirpatch, A.; Adolf, D. B. *Macromolecules* **2004**, *37*, 1576.
(34) Roland, C. M.; Paluch, M.; Pakula, T.; Casalini, R. *Philos. Mag.* **2004**, *84*, 1573.
(35) Ougizawa, T.; Dee, G. T.; Walsh, D. J. *Macromolecules* **1991**, *24*, 3834.
(36) Sun, T.; King, H. E. *Macromolecules* **1998**, *31*, 6383.
(37) Hammouda, B.; Ho, D.; Kline, S. *Macromolecules* **2002**, *35*, 8578.
(38) Smith, G. D.; Bedrov, D. *J. Phys. Chem. B* **2003**, *107*, 3096.
(39) Poole, P. H.; Sciortino, F.; Grande, T.; Stanley, H. E.; Angell, C. A. *Phys. Rev. Lett.* **1994**, *73*, 1632.

MA048585V